

# Photometric identification of emission line sources in the southern photometric local Universe survey (S-PLUS)

L. A. Gutiérrez-Soto,<sup>1</sup>★ Second Author,<sup>2</sup> Third Author<sup>2,3</sup> and Fourth Author<sup>3</sup>

<sup>1</sup>Departamento de Astronomia, IAG, Universidade de São Paulo, Rua do Matao, 1226, 05509-900, São Paulo, Brazil

<sup>2</sup>Department, Institution, Street Address, City Postal Code, Country

<sup>3</sup>Another Department, Different Institution, Street Address, City Postal Code, Country

Accepted XXX. Received YYY; in original form ZZZ

## ABSTRACT

The emission line objects are very important objects in astronomy because reflects different class of objects that evolved physical mechanics that given counts of formation stellar process, presences the gas, shocks, star-burst in galaxies, the finals stage of stars among others process. For this reason we have created a list of H $\alpha$  emitters selected from the S-PLUS data, which is mapping the southern hemisphere at relatively high latitudes. We implemented the (r - J0660) versus (r - i) color-color diagram for that task. We found 9,200 objects that exhibit um excess in emission in the J0660 which we have traduced as the presence of the H $\alpha$  emission line. In addition we have found that by combining the colors: (r - i) and (g - z) with unsupervised (clustering) machine learning it is possible separate our list of emitters in two sub-groups: one with intense blue continuum and another with intense red one.

**Key words:** keyword1 – keyword2 – keyword3

## 1 INTRODUCTION

The existence of an ionizing radiation field can lead to Balmer hydrogen emission lines. From the presence of the H Balmer lines in the optical spectra of some sources it is well known the possible presence of ionized gas. Many important astronomical objects involve the physics of photo-ionized gases and the interpretation of the emission-line spectra. Emission line objects as the H II regions allow us to study the star formation history of the far reaches of our Galaxy and of distant galaxies. Planetary nebulae let us to see the remaining envelope of dying stars. Star-burst galaxies and QSOs are one the most luminous objects and hence the most distant that can be observed. Their spectra can reveal details about of the first generation of star and the formation of heavy elements in the young universe. On the other hand, emission lines can also infer the presence or lack the accretion discs (Schwope et al. 2000; Ratti et al. 2012), the properties of single or double picked line can allow us to infer geometrical characteristics (Horne & Marsh 1986), the nature of donor stars in binary system (Steeghs & Casares 2002; van Spaandonk et al. 2010; Casares 2015) and the compact objects as black holes (Casares 2016).

Emission lines are also associated with stars in very early-type and/or very late evolutionary stage which are short phase. As already mentioned are also associated with binaries that experiencing mass transfer. These group of emission line stars includes young stellar (YSOs) and Herbig-Haro (HH) objects, post-asymptotic and some asymptotic giant branch (AGB), some red giant stars (RGB), Wolf-Rayet (WR) stars, supernova remnants, classical Be stars, active late-type dwarfs, interacting binary system like symbiotic stars

(SySt) and cataclysmic variables (CV). Most of these class of object are in-homogeneous and some contains many few identified members, for instance at the moment around 323 symbiotic system have been identified from which 257 belong to the Galaxy and ~66 are extra-galactic objects (Akras et al. 019a). The same occurs with PNe from witch around 3500 of them are been cataloged (Parker et al. 2016), this current number of PNe represents only about 15-30% of the estimated total of Galactic PNe (Frew, 2008; Jacoby et al., 2010) showing that a small fraction of the PNe have been cataloged. Many galaxies, in addition to harbor Planetary nebulae and H II regions, show characteristic nebular in their spectra. In most of these objects, the gas is photoionized by hot stars in the nucleus, which is thus much like giant H II region, or perhaps many H II regions. The galactic nucleus with very strongest emission lines of this type are often called blue compact galaxies, extragalactic H II regions, star forming or starburst galaxies (Osterbrock & Ferland 2006). There are also spiral galaxies that present emission lines.

In the past H surveys with modest spatial resolutions have been used to identified extended nebular emission to study supernova remnants, galaxy groups and star forming regions (Davies, Elliott Meaburn 1976). More recently, higher resolution surveys such as the INT Photometric H $\alpha$  survey (IPHAS; Drew et al. 2005; Barentsen et al. 2014) have focused in the study of compact emission line sources on the Galactic plane, typically with objects in different stage of stellar evolution. The Anglo-Australian Observatory UKS chmidt Telescope Supercosmos H $\alpha$  Survey (Parker et al. 2005) is another H $\alpha$  survey of the Southern Galactic Plane and Magellanic Cloud which has covered to b ~ 10-13° (verificar esto). Currently ongoing is the VST Photometric H $\alpha$  Survey of the Southern Galactic Plane and Bulge (VPHAS+; Drew et al. 2014) that will cover the Galactic bulge and plane in five filters.

\* E-mail: gsoto.angel@gmail.com

Like VPHAS+, others ongoing surveys that are used to study the population of emission line objects are the The Javalambre Photometric Local Universe Survey (J-PLUS<sup>1</sup>, Cenarro et al. 2018) and the Southern-Photometric Local Universe Survey (S-PLUS<sup>2</sup>, Mendes de Oliveira et al. 2019) are providing observations of the Galactic halo covering both northern and southern celestial hemispheres in a systematic way with twin telescopes using the same set of multi-band filters. In addition to the H $\alpha$  filter, which is already vastly applied to systematically searching for H $\alpha$  emitters the telescopes offer 11 more filters. And more ambitious yet the JPAS survey that will the same area of J-PLUS in 56 narrow-band filters.

Traditionally, color-color diagrams based in H $\alpha$  filter are been used to identify H $\alpha$  emitters. The analysis the color-color diagram ( $r - H\alpha$ ) versus ( $r - i$ ) has resulted on the discovered of new emission line objects, for instance Witham et al. (2006, 2007) used the ( $r - H\alpha$ ) versus ( $r - i$ ) colour-colour diagram to find for new CV. On the other hand, Vink et al. (2008) reported the discovery of YSOs by using this same colour criteria. In this sense using this methodology a variety of classes of objects are been identified, which include symbiotic stars (Corradi et al. 2008; Corradi & Giannanco 2010; Corradi et al. 2011), early type emission line stars (Drew et al. 2008) and planetary nebulae (Viironen et al. 2009; Sabin et al. 2010). Recently, by using this same color diagram were also identified compact PN candidates in VPHAS+ catalog (Akras et al. 2019). And the same diagram in conjunction with new ones shows to be very efficient to find for PN candidates (Gutiérrez-Soto et al. 2020). In general terms, Witham et al. (2006) presented a methodology and first results in looking for emission line sources in narrow-band surveys.

In this work, we used S-PLUS observations of the southern hemisphere to search for objects with an excess of H $\alpha$  using automatic methods based on the ( $r - H\alpha$ ) versus ( $r - i$ ) color-color diagram we also used color criteria based in ( $g - r$ ) and ( $z - g$ ) in conjunction to unsupervised machine learning techniques to split the final list in those with blue and red continuum. The paper is organized as follows...

## 2 OBSERVATIONS

Particularly, we are implemented data from S-PLUS DR3 (ref) to carried out our study. S-PLUS is 12-band optical photometric survey, which are formed by using seven narrow-band and five broad-band like SDSS filters. The narrow-band set include the filter  $J0660$  which detect the H $\alpha$  emission line. Figure 1 shows the Javalambre filter system (Marín-Franch et al. 2012) overlapping are the optical spectra of several class emission line objects on which it is possible to see that the H $\alpha$  line falls into the  $J0660$  filter, except for the QSOs.

The actual data release contains about 60 millions of objects covering a total area of  $\sim 8000 \text{ deg}^2$ , at high Galactic latitudes ( $> 30 \text{ deg}$ ) using a dedicated 0.83m robotic telescope, the T80-South (T80S), located at Cerro Tololo, Chile. S-PLUS will cover an additional  $1300 \text{ deg}^2$  of the Galactic plane and bulge to enable Galactic studies. In this work, we focus on the aspects that are of particular interest to the second data release of the S-PLUS main survey. Additional information about S-PLUS can be found in Mendes de Oliveira et al. (2019).

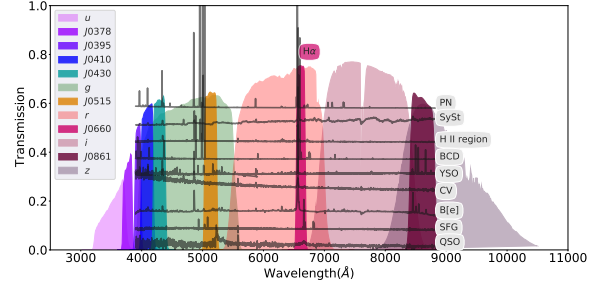


**Figure 1.** Transmission curves of the S-PLUS filters set. The narrow-band filter  $J0660$  detects the H $\alpha$  emission line. Over-plotted are different classes of emission line objects, from upper to down PN, SySt ...

## 3 METHODOLOGY

We first constructed a sub-sample from all S-PLUS DR3 from which we applied an iterative and automatic technique to select objects with an excess of H $\alpha$  emission line, as we describe below:

### 3.1 Initial selection sample

The first step in our selection procedure consist in the following criteria to guarantee the quality of the observations of the objects:

- (i) The sources must have detection in the filters:  $r$ ,  $i$  and  $J0660$ . To assure that we select object must have error minor or equal to 0.2 in each of three filter.
- (ii) Must have an  $r$  magnitude until  $r = 21$ .

### 3.2 Finding the main stellar locus and selecting the H $\alpha$ emitters

Once the initial cut were made, we proceed to select the objects with an excess of H $\alpha$  which is represent relatively high value of the filter  $J0660$  in comparison with  $r$ -band filter. For that we first divided our sub-sample in four magnitude bins using the  $r$ -band magnitudes. The bins have the follow distribution:

- 1 bin- objects with magnitude in the  $r$ -band  $r < 16$
- 2 bin- objects with magnitude in the  $r$ -band  $16 \leq r < 18$
- 3 bin- objects with magnitude in the  $r$ -band  $18 \leq r < 20$
- 4 bin- objects with magnitude in the  $r$ -band  $20 \leq r < 21$

To select the  $r - J0660$  color, Witham et al. (2008) presented a catalogue of point-sources H $\alpha$  emission objects identified in IPHAS.

To select the emission lines we used the same method created and implemented by Witham et al. (2008) its possible to do that because the S-PLUS has similar filters that the IPHAS project, which are  $r$ ,  $J0660$  and  $i$ . This technique was used by Scaringi et al. (2013) to identify blue objects with excess of H $\alpha$  and after that Wevers et al. (2017) also applied this methodology to create catalogue of candidate H $\alpha$  emission showing a high effectiveness. Applying the selection criteria to selecting H $\alpha$  emitters. We used the same procedure in Wevers et al. (2017). The objects with H $\alpha$  excess meet the condition:

$$(r - J0660)_{\text{obs}} - (r - J0660)_{\text{fit}} \geq C \times \sqrt{\sigma_s^2 - \sigma_{\text{phot}}^2} \quad (1)$$

where  $\sigma_s$  is the root mean squared value of the residuals around the fit and  $\sigma_{\text{phot}}$  is the error on the observed  $(r - J0660)$  colour

Firts see an approximation of the  $4\sigma$  cut away from the original fit.

In Figure 2 is illustrate the selection process. The black line represent the fit

<sup>1</sup> <https://www.j-plus.es>

<sup>2</sup> <http://www.splus.iag.usp.br>

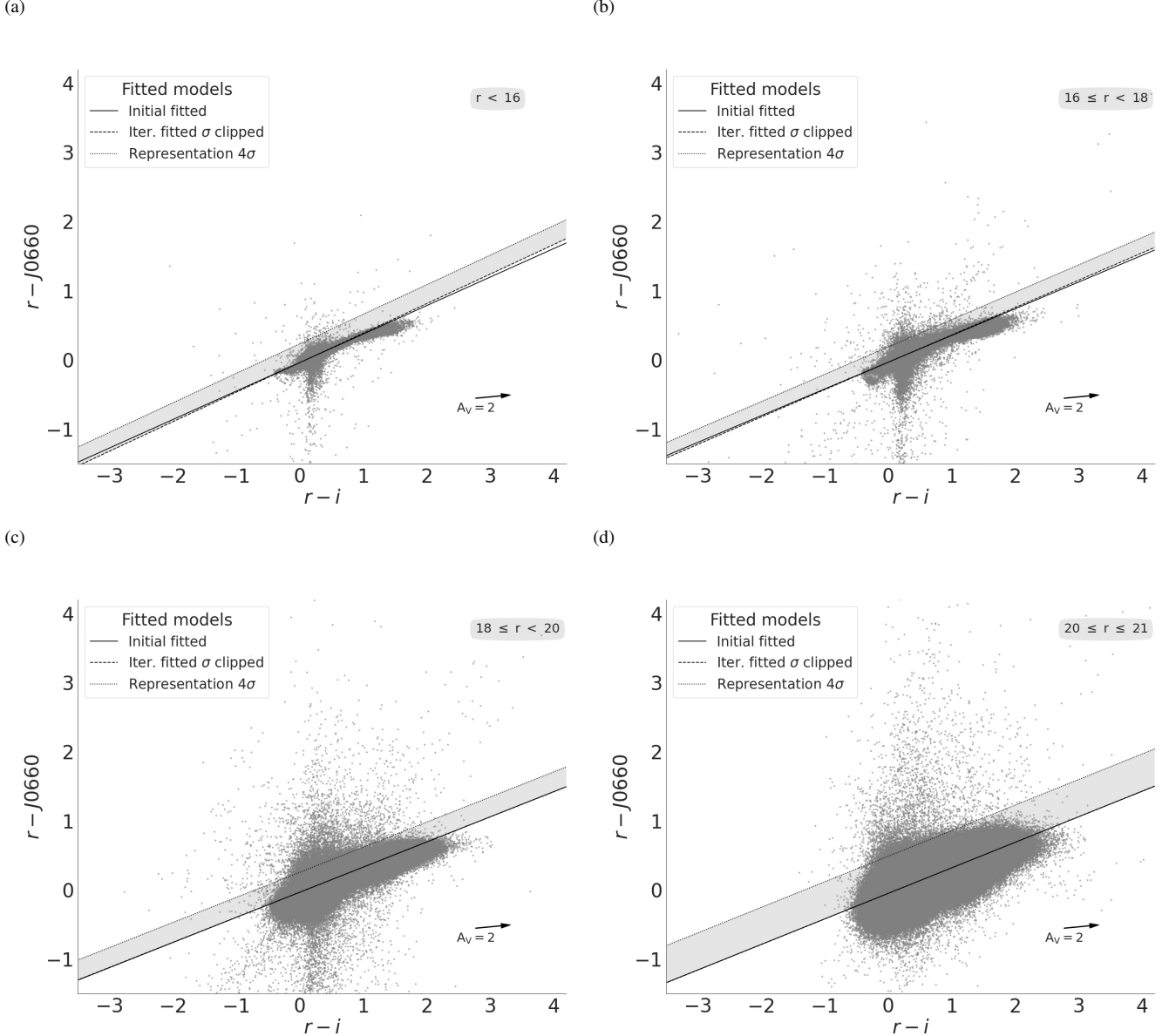


**Figure 2.** An illustration of the selection criteria used to identify strong emission-line objects via colour-colour plots. The data shown here are all from the S-PLUS DR3. The data are split up into four magnitude bins, as shown in the four panels. Objects with H $\alpha$  excess should be located near the top of the colour-colour plots. The thin red lines illustrate the original least-squares fit to all the data (grey points). The thin blue lines represent the final fits to the upper locus of points obtained by applying an iterative  $\sigma$ -clipping technique to the initial fit. The actual cuts used to select H $\alpha$  emitters are shown by the thick dashed lines. If the cut was based on the initial (final) fit, it is shown in red (blue). Objects selected as H emitters must be located above the cut and are shown as large triangles. Note that the cut lines shown here are only approximate, as the actual selection criterion also considers the errors on each individual data point. This explains, for example, why an object in the bottom right-hand panel is not selected despite clearly lying above the cut line.

### 3.3 Maths

### 3.4 Figures and tables

## 4 RESULTS

## 5 CONCLUSIONS

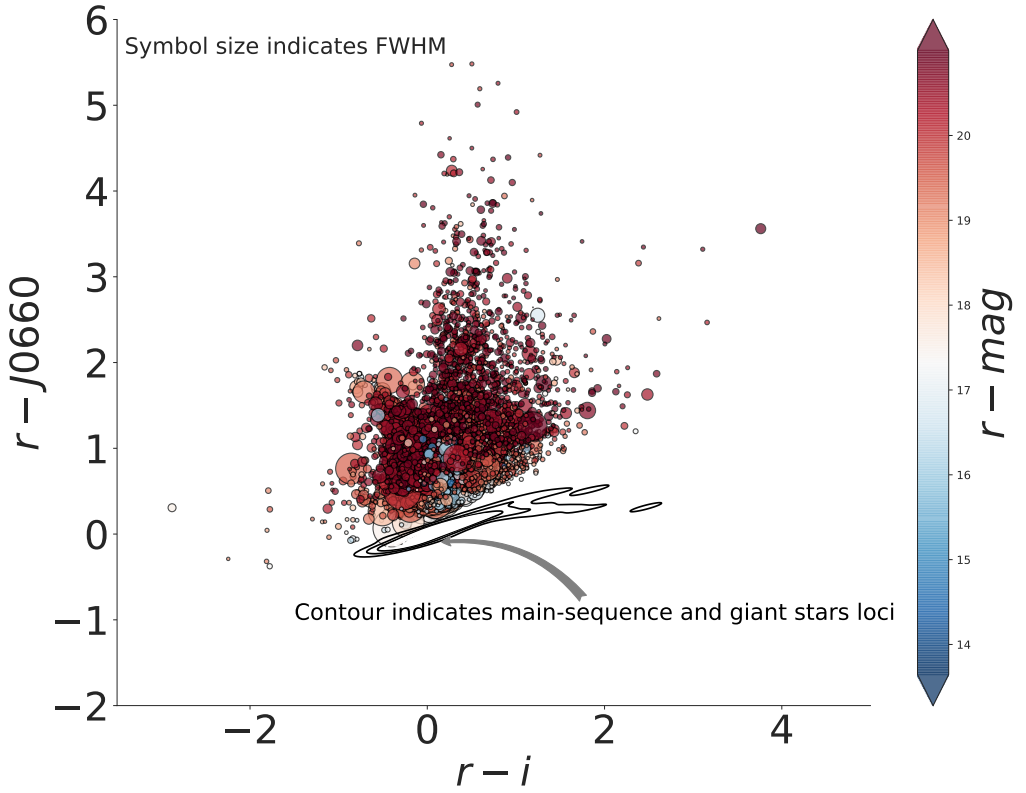
We have found a important sample of emission line objects.

## ACKNOWLEDGEMENTS

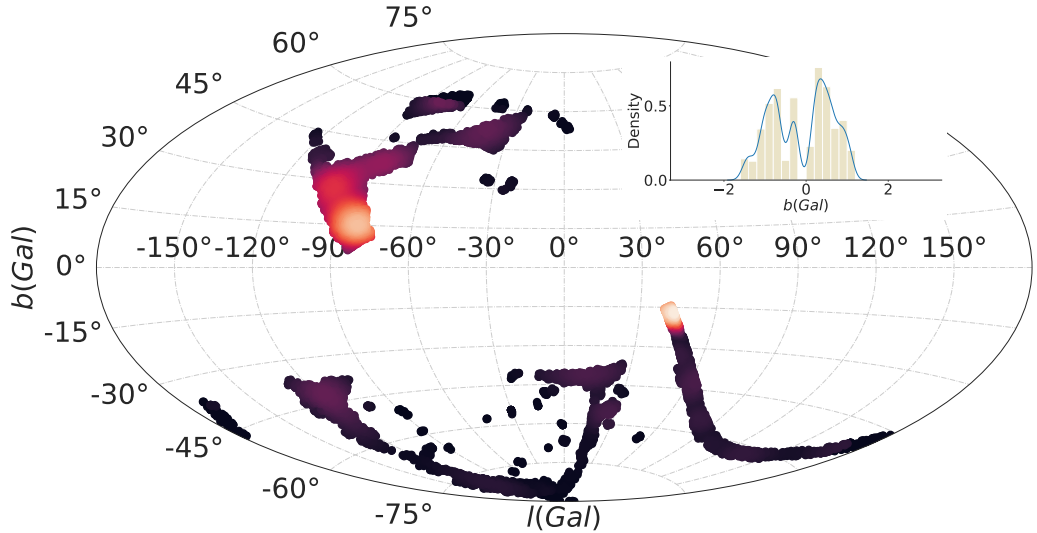
## DATA AVAILABILITY

## REFERENCES

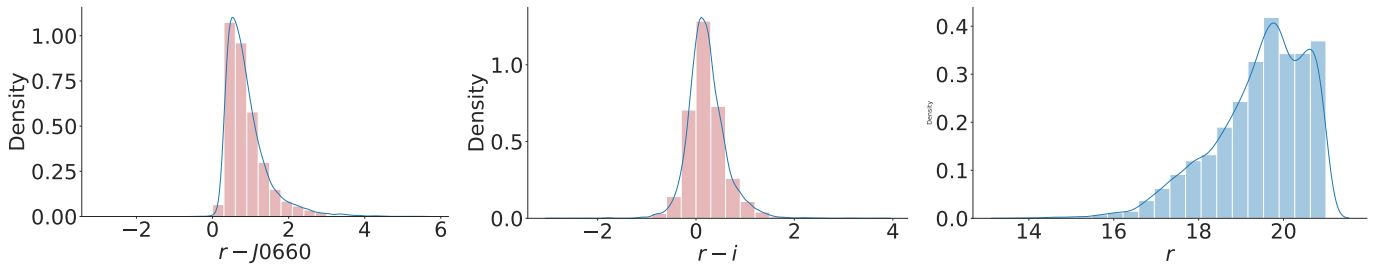
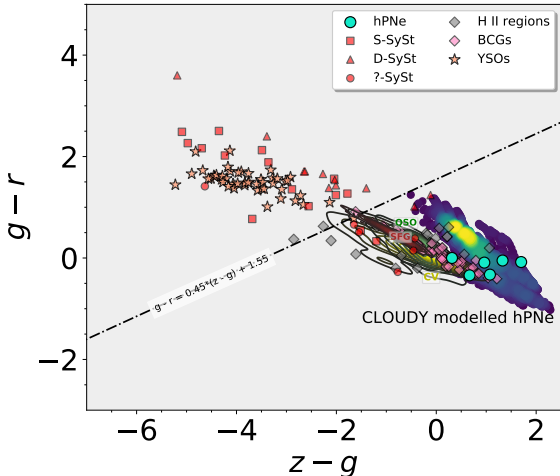
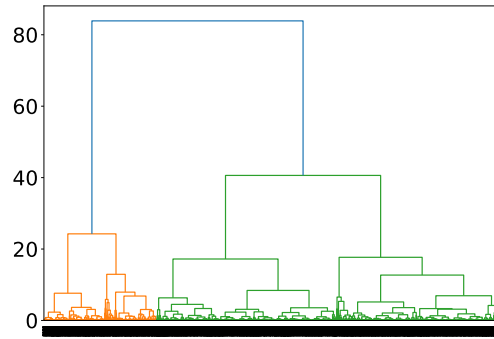
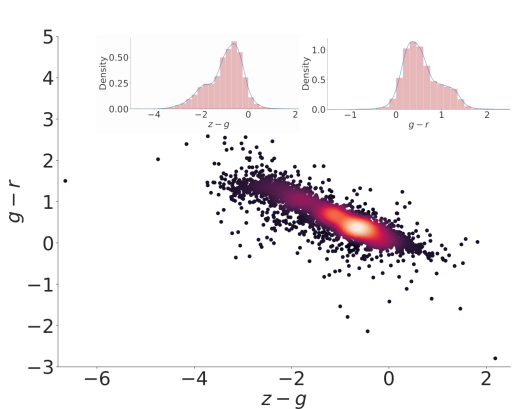
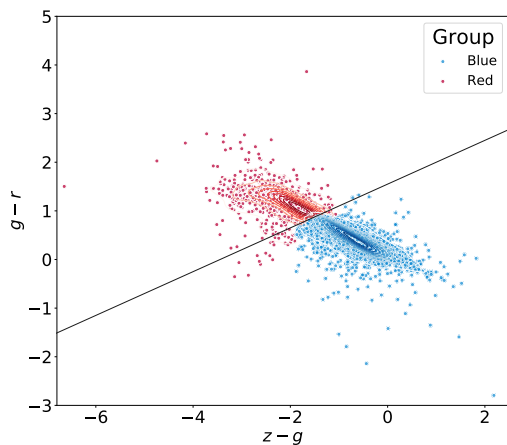
- Akras S., Guzman-Ramirez L., Gonçalves D. R., 2019, *MNRAS*, **488**, 3238
- Akras S., Guzman-Ramirez L., Leal-Ferreira M., Ramos-Larios G., 2019a, *ApJS*, **240**, 21
- Almeida-Fernandes F., et al., 2021, arXiv e-prints, p. [arXiv:2104.00020](https://arxiv.org/abs/2104.00020)
- Barentsen G., et al., 2014, *MNRAS*, **444**, 3230
- Casares J., 2015, *ApJ*, **808**, 80
- Casares J., 2016, *ApJ*, **822**, 99



**Figure 3.** Colour-colour diagram with all the emission line objects selected from S-PLUS DR3. Size of the symbols represent the measured FWHM assuming a Gaussian core (for more detail see Almeida-Fernandes et al. 2021). Colored bar is the magnitude values in the r-band. The contours represent the synthetic main-sequence and giant stars loci from the library of stellar spectral energy distributions of Pickles (1998).



**Figure 4.** This is my embedded figure

**Figure 5.** Emission lines selected...**Figure 6.** Classifying...**Figure 8.** Costomer dendrogram...**Figure 7.** Classifying...**Figure 9.** Costomer dendrogram...

- Cenarro A. J., et al., 2018, preprint, ([arXiv:1804.02667](https://arxiv.org/abs/1804.02667))  
 Corradi R. L. M., Giannanco C., 2010, *A&A*, **520**, A99  
 Corradi R. L. M., et al., 2008, *A&A*, **480**, 409  
 Corradi R. L. M., Sabin L., Munari U., Cetrulo G., Englaro A., Angeloni R., Greimel R., Mampaso A., 2011, *A&A*, **529**, A56  
 Drew J. E., et al., 2005, *MNRAS*, **362**, 753  
 Drew J. E., Greimel R., Irwin M. J., Sale S. E., 2008, *MNRAS*, **386**, 1761  
 Drew J. E., et al., 2014, *MNRAS*, **440**, 2036  
 Gutiérrez-Soto L. A., et al., 2020, *A&A*, **633**, A123  
 Horne K., Marsh T. R., 1986, *MNRAS*, **218**, 761  
 Mendes de Oliveira C., et al., 2019, *MNRAS*, **489**, 241

- Osterbrock D. E., Ferland G. J., 2006, *Astrophysics Of Gas Nebulae and Active Galactic Nuclei*. Sausalito: University Science Books, <https://books.google.com.br/books?id=HgfrkDjBD98C>  
 Parker Q. A., Bojić I. S., Frew D. J., 2016, in *Journal of Physics Conference Series*. p. 032008 ([arXiv:1603.07042](https://arxiv.org/abs/1603.07042)), doi:10.1088/1742-6596/728/3/032008  
 Pickles A. J., 1998, *PASP*, **110**, 863  
 Ratti E. M., Steeghs D. T. H., Jonker P. G., Torres M. A. P., Bassa C. G., Verbunt F., 2012, *MNRAS*, **420**, 75

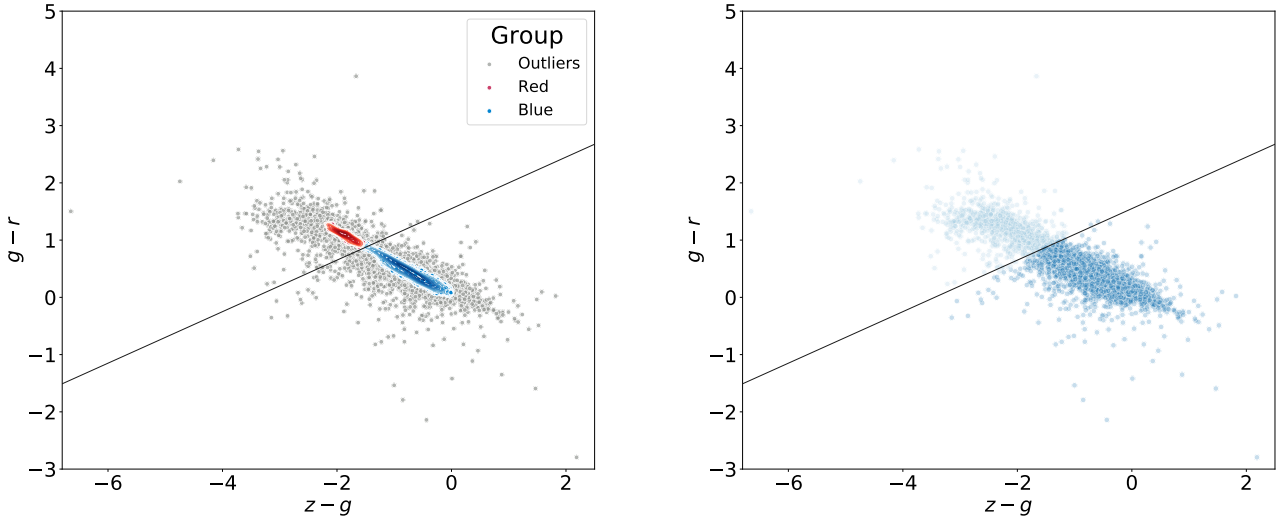
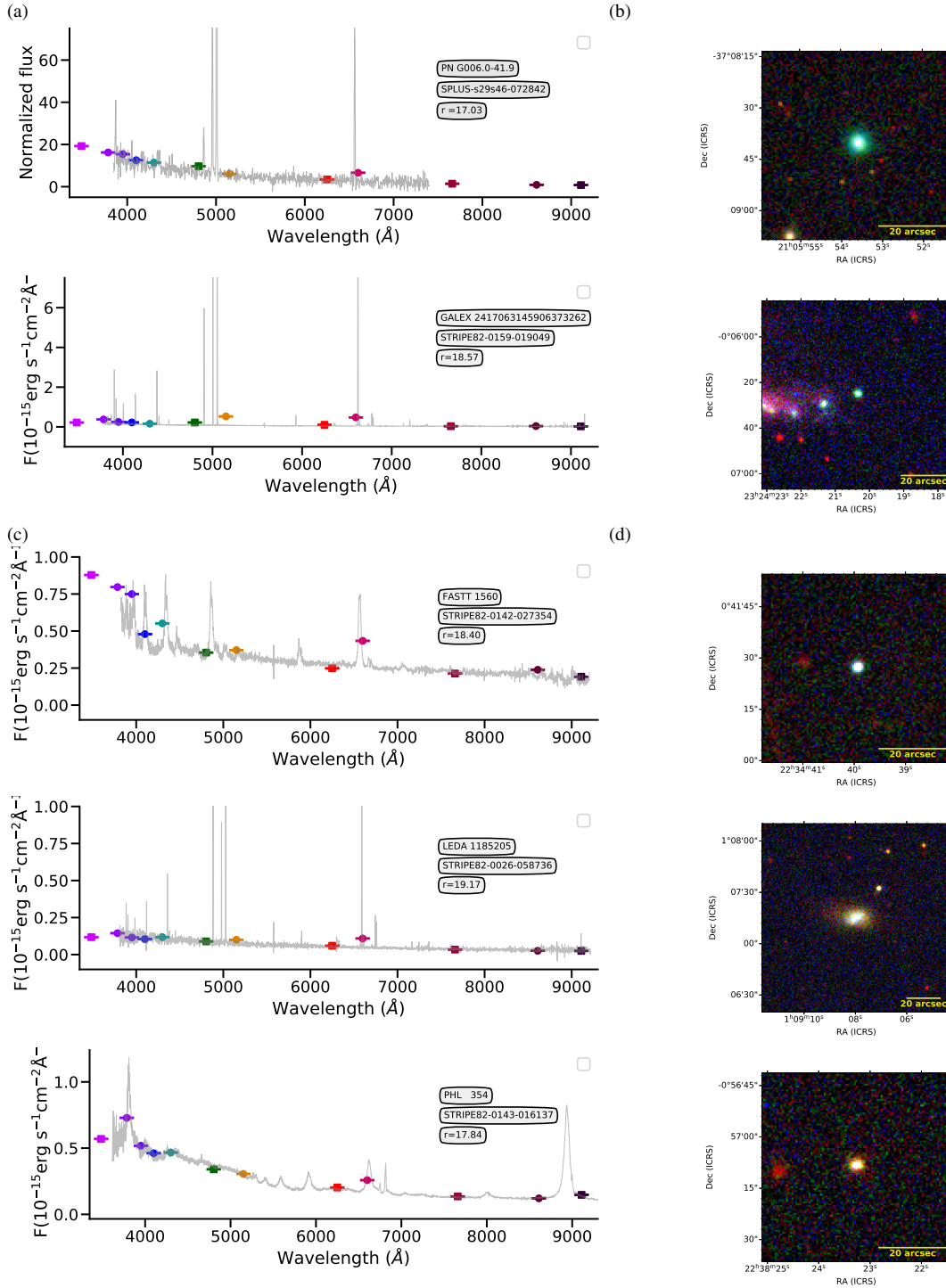


**Figure 10.** New color-color diagram to separate the blue objects from the red ones.

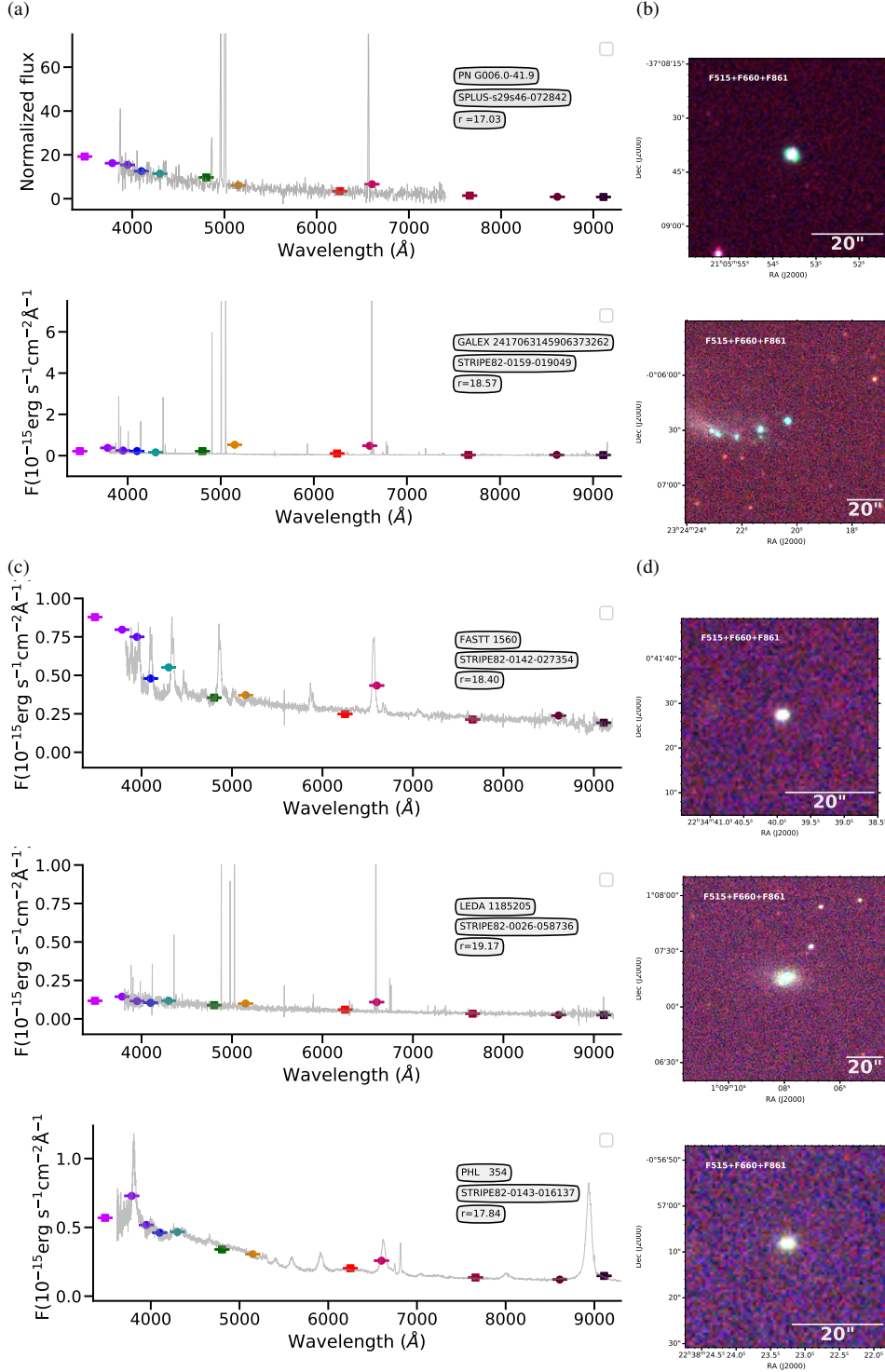
- Sabin L., Zijlstra A. A., Wareing C., Corradi R. L. M., Mampaso A., Viironen K., Wright N. J., Parker Q. A., 2010, [Publ. Astron. Soc. Australia](#), **27**, 166  
 Scaringi S., Groot P. J., Verbeek K., Greiss S., Knigge C., Körding E., 2013, [MNRAS](#), **428**, 2207  
 Schwope A. D., Catalán M. S., Beuermann K., Metzner A., Smith R. C., Steeghs D., 2000, [MNRAS](#), **313**, 533  
 Steeghs D., Casares J., 2002, [ApJ](#), **568**, 273  
 Viironen K., et al., 2009, [A&A](#), **502**, 113  
 Vink J. S., Drew J. E., Steeghs D., Wright N. J., Martin E. L., Gänsicke B. T., Greimel R., Drake J., 2008, [MNRAS](#), **387**, 308  
 Wevers T., et al., 2017, [MNRAS](#), **466**, 163  
 Witham A. R., et al., 2006, [MNRAS](#), **369**, 581  
 Witham A. R., et al., 2007, [MNRAS](#), **382**, 1158  
 Witham A. R., Knigge C., Drew J. E., Greimel R., Steeghs D., Gänsicke B. T., Groot P. J., Mampaso A., 2008, [MNRAS](#), **384**, 1277  
 van Spaandonk L., Steeghs D., Marsh T. R., Torres M. A. P., 2010, [MNRAS](#), **401**, 1857

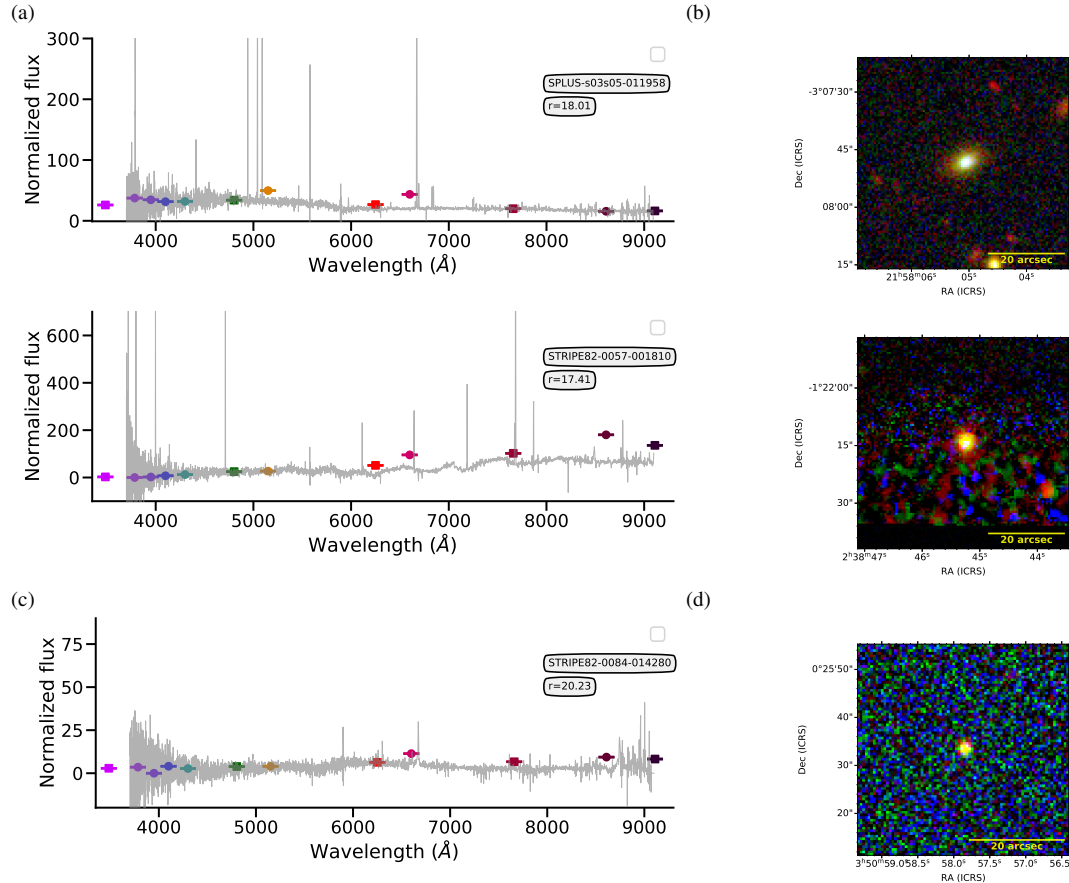
## APPENDIX A: SOME EXTRA MATERIAL

This paper has been typeset from a  $\text{\TeX}/\text{\LaTeX}$  file prepared by the author.

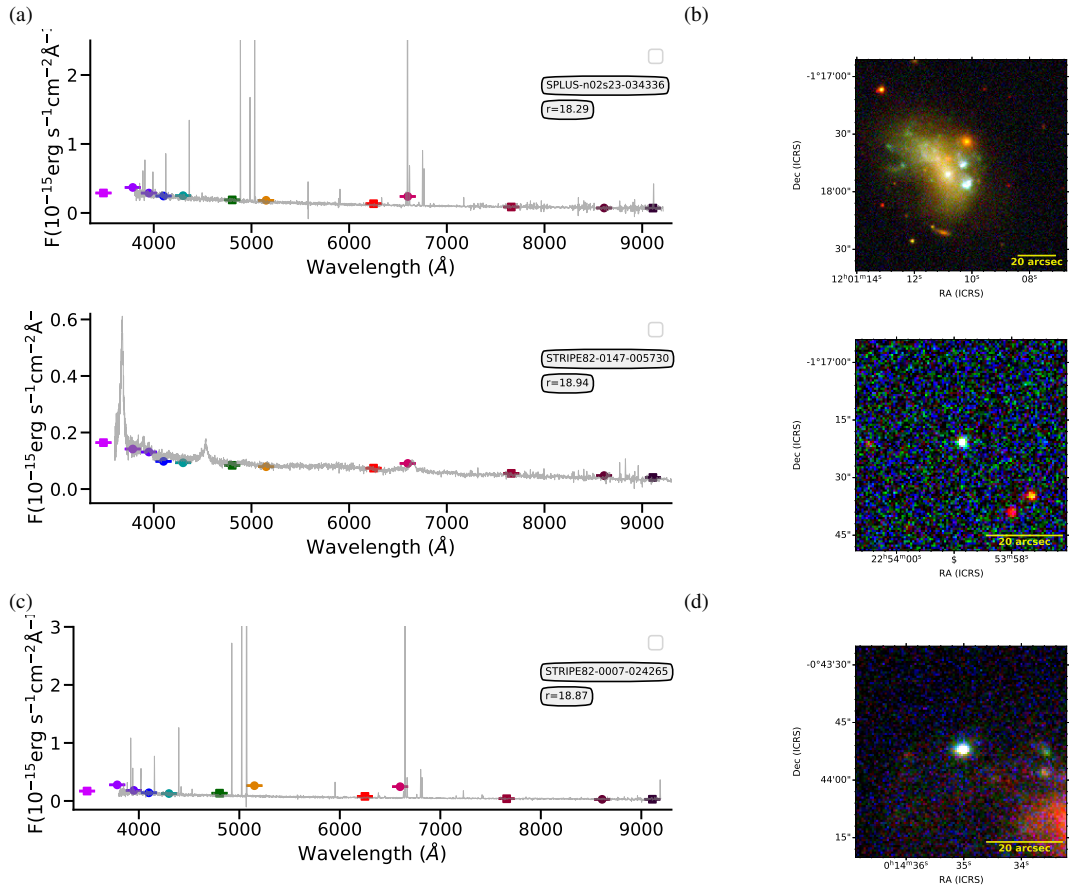


**Figure 11.** Spectra of the known objects select with our algorithm

**Figure 12.** Spectra of the known objects select with our algorithm



**Figure 13.** Spectra of the Lamost

**Figure 14.** Spectra of the SDSS